

# **Method to determine full work of fracture from disk shaped compact tension tests on hot-mix asphalt**

**E. Denneman**

CSIR Built Environment, PO Box 395 Pretoria, 0001, South Africa, edenneman@csir.co.za

## **ABSTRACT**

Fatigue cracking is an important mode of failure in hot-mix asphalt (HMA). As part of the revision of the South African pavement design method (SAPDM) a need was identified to assess the fracture toughness of HMA in terms of fracture energy. The disk shaped compact tension test (DSCTT) was selected to experimentally determine the fracture energy. The paper contains the results of an initial round of testing aimed at assessing the suitability of the DSCTT procedure for use in the SAPDM project. The study found that when the DSCTT is performed in accordance with the ASTM test method, a portion of the work of fracture will not be recorded. A methodology is proposed to model the missing part of the exponential tail of the DSCTT load displacement curve and in doing so obtain a more precise measure of the work of fracture and therefore the fracture energy. Numerical simulation using the embedded discontinuity method shows that the value for fracture energy obtained from the DSCTT can be used to accurately reproduce the fracture behaviour of the material.

From the proceedings of the 29<sup>th</sup> Southern African Transport Conference (SATC 2010)

16-19 August 2010, Pretoria, South Africa, Page 465-474

ISBN: 978-1-9200017-47-7

# Method to determine full work of fracture from disk shaped compact tension tests on hot-mix asphalt

E. Denneman

CSIR Built Environment, PO Box 395 Pretoria, 0001, South Africa, edenneman@csir.co.za

## ABSTRACT

Fatigue cracking is an important mode of failure in hot-mix asphalt (HMA). As part of the revision of the South African pavement design method (SAPDM) a need was identified to assess the fracture toughness of HMA in terms of fracture energy. The disk shaped compact tension test (DSCTT) was selected to experimentally determine the fracture energy. The paper contains the results of an initial round of testing aimed at assessing the suitability of the DSCTT procedure for use in the SAPDM project. The study found that when the DSCTT is performed in accordance with the ASTM test method, a portion of the work of fracture will not be recorded. A methodology is proposed to model the missing part of the exponential tail of the DSCTT load displacement curve and in doing so obtain a more precise measure of the work of fracture and therefore the fracture energy. Numerical simulation using the embedded discontinuity method shows that the value for fracture energy obtained from the DSCTT can be used to accurately reproduce the fracture behaviour of the material.

## 1. INTRODUCTION

Cracking is a major form of distress occurring in hot-mix asphalt (HMA) road pavement layers. Cracks may result from: fatigue fracture propagation under repeated traffic loading, brittle fracture at low temperatures, reflective cracking from underlying layers, or any combination of these causes. Once cracks have propagated to the surface of the pavement, water can penetrate the structure, which in many cases leads to an acceleration of damage accumulation, often resulting in potholes.

In current South African design practise the cracking propensity of HMA is assessed to some extent with the indirect tensile test (ITS) in accordance with TMH1-C12T and for more advanced designs using the four point beam fatigue test.

As part of the revision of the South African pavement design method (SAPDM), a need was identified to assess the fracture toughness of HMA in terms of its fracture energy  $G_f$ . For this purpose a test method known as the disk shaped compact tension test (DSCTT) was selected. The DSCTT was developed by Wagoner et al (2005), and now available as standard test method ASTM D7313-07a.

The fracture energy  $G_f$  could prove to be a useful design parameter, as it can be used in fracture mechanics based analysis of crack propagation in pavements. When both the  $G_f$  and tensile strength  $f_t$  of the material are known the cracking behaviour of the material can be modelled using fracture mechanics approaches such as the cohesive crack model as

introduced by Hillerborg et al (1976) for concrete. In the cohesive model, a crack is induced when the stress in the material reaches  $f_t$ . After the crack has formed, stresses will still be transferred over the crack (e.g. through aggregate interlock), but the amount of stress transferred reduces as the crack width increases. Figure 1a shows the behaviour of model for a material that responds in a linear elastic manner before fracture. Once the stress has reached the value of  $f_t$  following a linear elastic path, a crack is formed. After crack induction the stress  $\sigma$  transferred across the crack may be written as a softening function of the crack width  $w$ :

$$\sigma = f(w) \quad (1)$$

The resulting softening function is shown in Figure 1b. The area underneath the softening curve is equal to  $G_f$ .

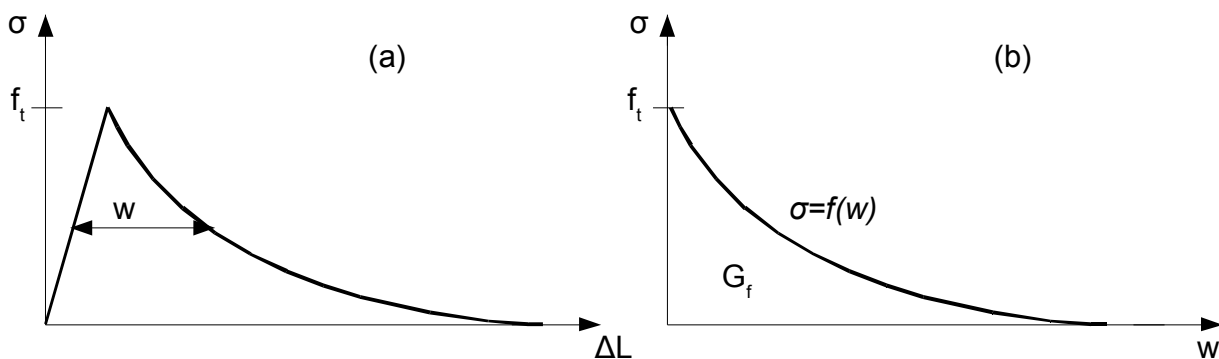


**Figure 1: Cohesive softening**

The cohesive crack approach can be used numerically to simulate the results of the DSCTT as shown by Wagoner et al (2005), Kim et al (2009) and in a previous paper presented at this conference by Denneman et al (2009).

This paper contains the results of an explorative round of DSCTT testing. The goal of the study is to assess the suitability of the DSCTT test method in ASTM D7313-07a for use as part of the SAPDM project and to adapt the procedure where required. The paper proposes an alteration to the calculation procedure to obtain  $G_f$  currently contained in ASTM D7313-07a.

To assess whether the obtained value for  $G_f$  from the DSCTT is accurate, the result is used to simulate the DSCTT numerically as part of this paper.

## 2. FRACTURE EXPERIMENTS

The tests were performed on a medium continuous mix with an SBS modified AE2 binder. The material was short term aged and compacted by means of the slab compactor following the methodology discussed in Anochie-Boateng et al (2010). Nine specimens were cored from slabs. After density determination, the specimens were cut to the dimensions for the DSCTT, as shown in Figure 2a and Table 1. The nominal thickness  $t$  of the specimens was 60 mm. The air void content of the cores as determined using the corelok apparatus (Anochie-Boateng et al, 2010) was 5.8 per cent with a standard deviation of 0.3 per cent.

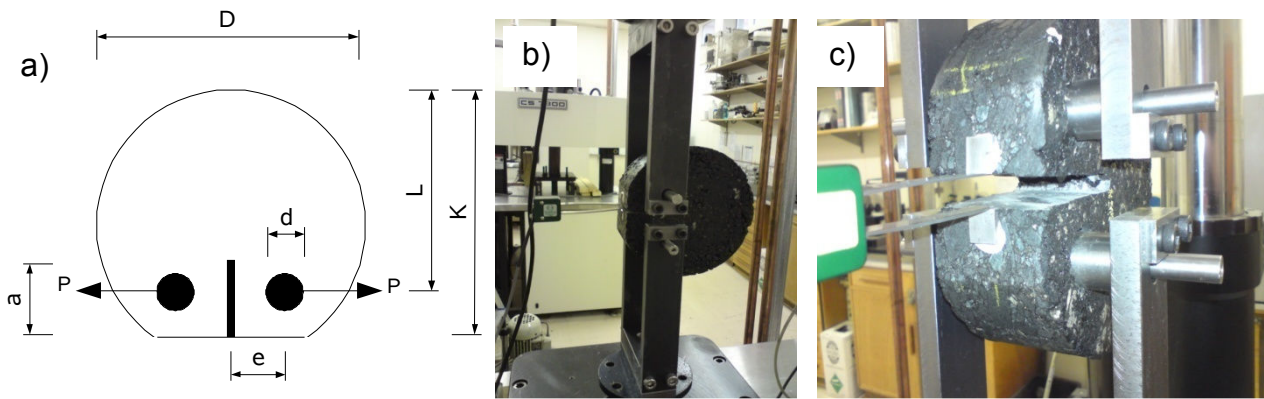


**Figure 2: a) Specimen dimensions DSCTT, b) Testing rig with specimen, c) Clip gauge recording crack mouth opening displacement (CMOD) during test.**

**Table 1: Dimensions of DSCTT specimens**

Dimension	[mm]
a	70
d	25
D	150
e	25
L	110
K	145

The tests were run in accordance with ASTM D7313-07a. The chosen test temperature was 5°C. Fracture tests are often run at low temperatures as asphalt is more prone to cracking at these temperatures. As part of the SAPDM project, fatigue and monotonic fracture tests will be performed in the 5°C to 20°C range. This was established to be the typical low temperature regime South African pavements are subjected to, using the pavement temperature prediction models published by Denneman (2007). The tests performed as part of this study were run at 5°C. Pictures of the testing rig and the mounted clip gauge, recording the crack mouth opening displacement (CMOD) during the test, are shown as Figure 2b and Figure 2c respectively. The results can be interpreted by plotting the load applied to fracture the specimen in tension against the CMOD. Figure 3 shows the load-CMOD curves for the nine specimens tested in this study. The test is performed in displacement control, at a constant speed of 0.017 mm/s. This speed proved too slow for the servo valve in its current setting, resulting in the step wise load application visible in Figure 3. The issue with the load application will have to be remedied as part of the protocol development for SAPDM.

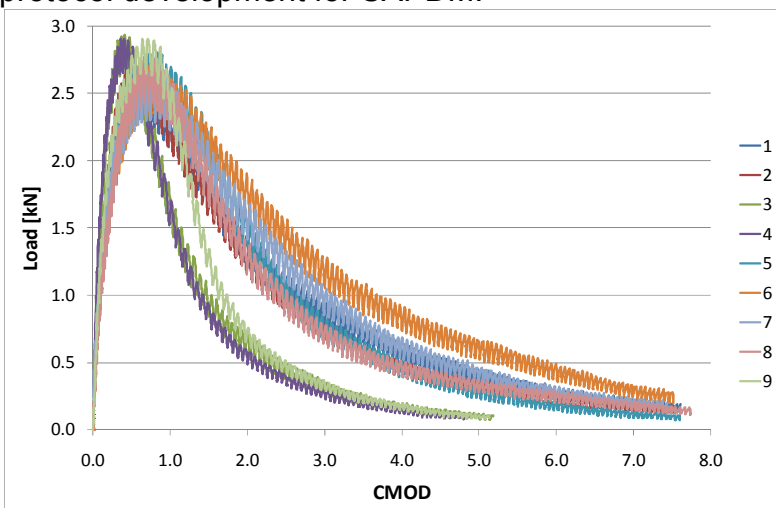


**Figure 3: Load-CMOD curves for DSCTT experiments at 5°C.**

### 3 CALCULATING THE FRACTURE ENERGY

The work  $W_f$  required to fracture the sample is represented by the area under the load-CMOD curves in Figure 3. The specific fracture energy  $G_f$  is equal to  $W_f$  per unit cracked area. For the DSCTT  $G_f$  is obtained from:

$$G_f = \frac{W_f}{t(K-a)} \quad (2)$$

This equation is only valid if all the work required to grow a crack over the distance  $K-a$  is recorded. The challenge in determining the work required to completely fracture the sample is that a piece of the exponential tail part of the curve will invariably be missing (refer Figure 3). This is due to the boundary conditions of the test and limitations to the measuring equipment. If  $G_f$  is calculated according to the procedures in ASTM D7313-07a, the work of fracture under the tail is ignored.

The missing tail is not specific to the DSCTT, but is also an issue when interpreting fracture tests performed on beams. The error in the determination of  $G_f$  due to the missing part of the curve can be significant. Elices et al (1992) developed a method to model the missing part of the load-displacement tail in weight corrected three point bending tests. The approach developed for beam tests by these researchers is amended in this paper to determine the full shape of the load displacement curve for the DSCTT.

At the end of the test when the crack has propagated to the very top of the sample and the load is approaching zero, the balance of forces in the specimen can be approached with the model shown in Figure 4. In this situation the specimen consists of two ridged pieces rotating around hinge point  $p$ . The remaining resistance against fracture propagation is offered by a cohesive tensile softening zone near the top of the sample. The angle of rotation  $\beta$  can be obtained from the CMOD reading using:

$$\beta = 2\varphi \quad (3)$$

Where:

$$\varphi = \tan^{-1} \left( \frac{\text{CMOD}}{2K} \right) \quad (4)$$

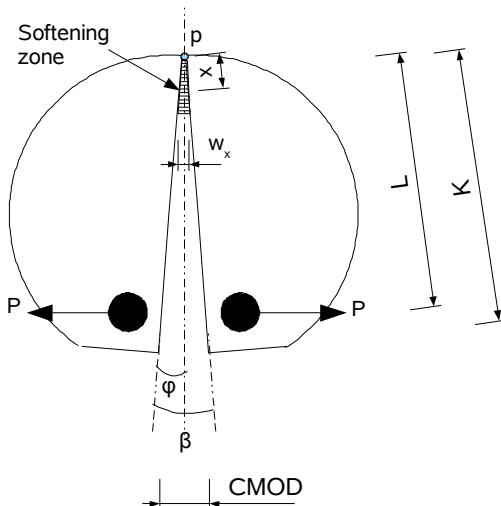


Figure 4: Kinematic model of disk near end of test

The crack width  $w_x$  at any distance  $x$  from point  $p$  can be calculated using:

$$w_x = 2x \sin \beta \quad (5)$$

When  $w_x$  is known, the crack bridging stress at any position in the softening zone can be calculated from the cohesive crack relationship in Equation 1. Following the example provided by Elices et al (1992) it can be shown that the moment capacity around  $p$  offered by the tension softening zone at the end of the test may be written as:

$$M = \frac{\alpha t G_f^2}{f_t(\beta)^2} \quad (6)$$

In this equation  $\alpha$  is a fitting parameter, which is dependent on the shape of the softening curve.  $\alpha$  is 1 for exponential softening, and 2/3 for linear softening. Equation 6 may be simplified to:

$$\frac{M}{t} = \frac{A}{\beta^2} \quad (7)$$

where

$$A = \frac{\alpha G_f^2}{f_t} \quad (8)$$

From Equation 7 follows that parameter  $A$  is the slope in plots of the moment around hinge point  $p$  per unit area ( $M/t$ ) versus  $\beta^{-2}$ . The results for the experiments performed as part of this is shown in Figure 5. The moment  $M$  around hinge point  $p$  due to external loading is:

$$M = PL \quad (9)$$

As can be seen from Figure 5 parameter  $A$  tends toward a constant for a certain material at large angles of rotation. Elices (1992) found  $A$  to be size independent for plain concrete. Size effect experiments would have to be conducted to investigate whether the same holds for HMA.

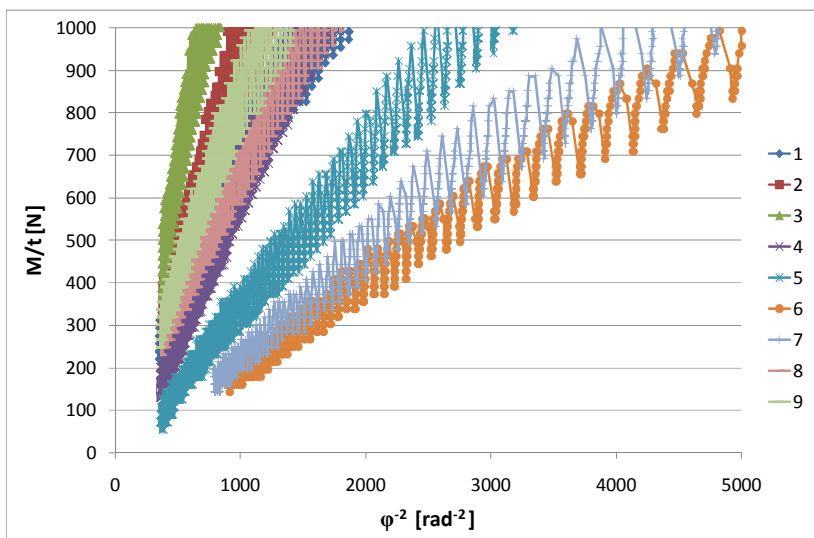


**Figure 5: Finding  $A$  for DSCTT results**

With  $A$  known, the load displacement curves can be extended by calculating the load  $P_{tail}$  at any value of  $\beta$  beyond the range for which data points are available. Combining Equations 7 and 9 allows:

$$P_{tail} = \frac{At}{L\beta^2} \approx \frac{AK^2t}{CMOD^2L} \quad (10)$$

The tail part of the load-CMOD curve can now be fitted as shown in Figure 6.

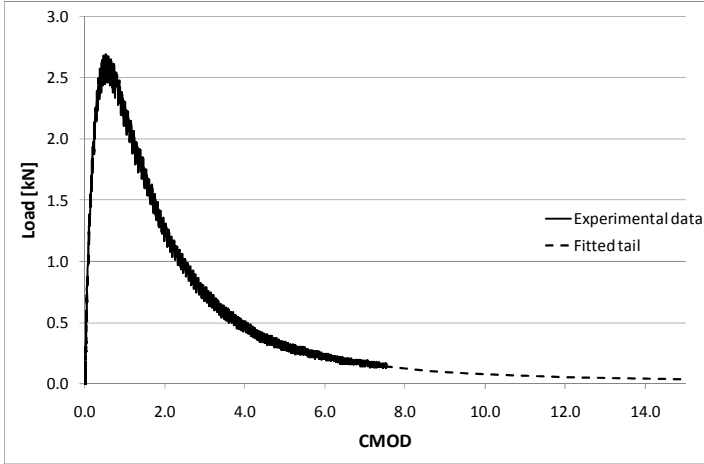


**Figure 6: Load CMOD curve with modelled tail.**

Finally the work of fracture (the area) under the modelled tail  $W_{tail}$  can be obtained from integrating 10 over the domain between the last recorded valid CMOD data point ( $CMOD_{max}$ ) and infinity:

$$W_{tail} = \int_{CMOD_{max}}^{\infty} P_{tail} d(CMOD) = \int_{CMOD_{max}}^{\infty} \frac{AK^2t}{CMOD^2L} d(CMOD) = \frac{AK^2t}{CMOD_{max} \cdot L} \quad (11)$$

The total fracture energy  $W_f$  can now be calculated by adding  $W_{tail}$  to the measured part of the work of fracture  $W_{measured}$ . The average results of the test in terms of  $W_f$  and calculated  $G_f$  are shown in Table 2. According to the model the fracture energy is underestimated by 12.6 per cent if the tail is not taken into account for the samples under study.

**Table 2: Summary of results (at 5°C)**

	Peak load [kN]	$W_{measured}$ [Nmm]	$W_{tail}$ [Nmm]	$W_f$ [Nmm]	$G_f$ [N/mm]
Average	2.81	6162	887	7049	1.61
Standard deviation	0.16			1879	0.45
Coefficient of variation	5.6%			26.7%	27.9%

#### 4 NUMERICAL SIMULATION

To assess whether the value obtained for  $G_f$  is accurate, the result is used to simulate the DSCTT numerically. The simulation is performed using the embedded discontinuity method (EDM) developed by Sancho et al (2007). Wu et al (2009) implemented the EDM in the open source finite element framework OpenSees (OpenSees, 2008), which is used for the numerical simulation in this paper. The software was used to model the DSCTT in a previous paper at this conference by Denneman et al (2009a). The EDM approach has further been applied to study fracture mechanics size effect in high performance concrete pavement materials (Denneman et al, 2009b). An advantage of the embedded

discontinuity method over more conventional cohesive crack methods is that it allows cracks to propagate independent of nodal positions and element boundaries.

The two dimensional numerical model of the DSCTT shown in Figure 7a is formed mainly of triangular elastic bulk elements. These elements require Young's modulus of elasticity and Poisson's ratio as input. Young's modulus was set to 10 GPa for the simulation based on the results at 0.1 Hz of the complex modulus tests performed on the material. Poisson's ratio is assumed to be 0.35. A narrow band of triangular shaped embedded discontinuity elements is provided at the notch facilitating a vertical crack path to the top of the sample. The embedded discontinuity elements provide the fracture response shown in Figure 1. Apart from fracture energy  $G_f$ , calculated in the previous section, the tensile strength  $f_t$  of the material needs to be known to model the tensile softening behaviour. An approximation of  $f_t$  was obtained from indirect tensile strength (ITS) testing in accordance with TMH 1-C12T. Five specimens were tested, the average  $f_t$  obtained was 3.62 MPa with a standard deviation of 0.21 MPa. The post crack tensile behaviour of the EDM elements was defined as function of crack width  $w$  using the exponential softening relation shown as Equation 12. The resulting softening function is shown in Figure 7b.

$$\sigma = f_t e^{(-aw)} \quad (12)$$

where:

$$a = \frac{f_t}{G_f} \quad (13)$$

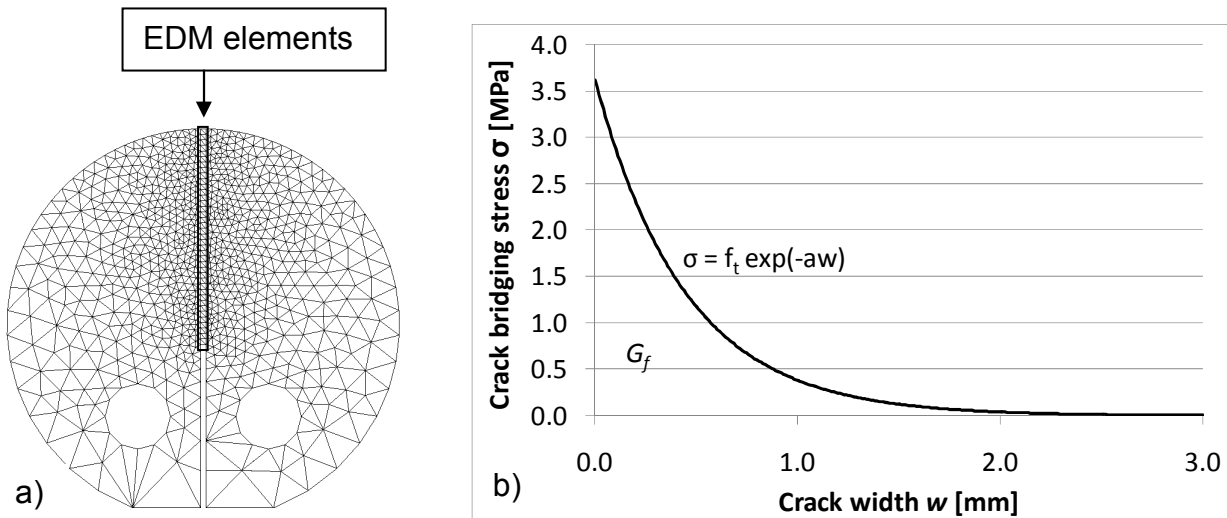


**Figure 7: a) FEM mesh with EDM elements, b) Cohesive softening function.**

The result of the numerical simulation compared to the load-CMOD curves obtained from the experiments is shown in Figure 8. A best fit to data was found when  $f_t$  was reduced to 70 per cent of the value determined in the ITS tests, while  $G_f$  was kept constant. Such calibration is common in literature; it is however an issue that needs to be addressed in the protocol development as part of the SAPDM project.

The tensile splitting method on which the ITS test is based, was originally developed for plain concrete. The equation to calculate  $f_t$  in the method comes from the continuum mechanics solution for the tensile stress in the centre of a circular section loaded by two point loads, offered by Timoshenko and Goodier (1970). The method is known to overestimate the tensile strength of plain concrete by up to 40 per cent (Olesen and Stang, 2006). This is due to size effects (Rocco, 1999a), (Rocco, 1999b), (Rocco, 2001). As well



as the difference in boundary conditions between the point loads in the original model by Timoshenko and Goodier and the actual boundary conditions provided by the loading strips with a certain width used in the splitting tests (Tang, 1994). It is reasonable to assume that some of the sources of error of the splitting test on concrete also hold relevance to the ITS test on HMA samples.

An additional possible source of the mismatch between the results of the DSCTT and the ITS results, is the speed at which the tests are performed. The ITS is standard run at the standard 50 mm per minute displacement, while the DSCTT is run at a speed of only 0.017 mm per second. The speed at which the tensile stress in the material increases in the two tests will be different.

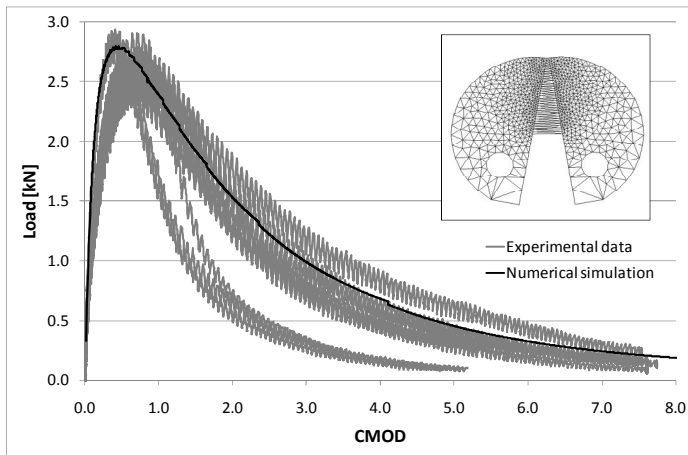


**Figure 8: Comparison of experimental and numerical results.**

## 5 CONCLUSIONS AND RECOMMENDATIONS

The objective of the paper is to assess the suitability of the DSCTT test method in ASTM D7313-07a for use as part of the SAPDM project and to adapt the procedure where required.

When the DSCTT is performed in accordance with the ASTM standard test method, a portion of the work of fracture required grow a crack through the entire ligament area will not be recorded. The missing part of the exponential tail of the load-CMOD curve can be modelled using the methodology provided in this paper. The results indicate that 12.6 per cent of the fracture energy would have been omitted if the missing tail was not modelled for the material under study. It is recommended that the methodology to model the tail of the test become part of the SAPDM test protocol for the DSCTT.

Numerical simulation of the experiments show that the obtained value of  $G_f$  can be used to accurately predict the fracture response of the material.

A study needs to be undertaken on the accuracy of the ITS test. It is expected that boundary conditions, size effect and load rate need to be corrected for, if the resulting tensile strength value is to be used with confidence in mechanistic pavement design models.

The issue with the irregular, step wise load application by the equipment used for the DSCTT needs to be resolved before testing as part of the revision of SAPDM is done.

## REFERENCES

ASTM D7313-07a, 2007. Determining Fracture Energy of Asphalt-Aggregate Mixtures Using the Disk-Shaped Compact Tension Geometry. ,ASTM.

Anochie-Boateng, J., Denneman, E., Mturi, G., O'Connell, J., Ventura, D., 2010. Hot mix asphalt testing for the South African pavement design method. Proceedings of the 30th Southern African Transport Conference. Pretoria.

Denneman, E., 2007. The application of locally developed pavement temperature prediction algorithms in performance grade (PG) binder selection. Proceedings of the 26th Southern African Transportation Conference, pp. 257-266.

Denneman, E., Wu, R., Kearsley, E. P., Visser, A. T., 2009a. Fracture mechanics in pavement design. Proceedings of the 29th Annual Southern African Transportation Conference. Pretoria.

Denneman, E., Kearsley, E., Visser, A. 2009b. Size-effect in high performance concrete road pavement materials. In Van Zijl, G. and Boshoff, W. (eds). Advances in cement-based materials, pp. 53-58, CRC Press, London.

Elices, M., Guinea, G., Planas, J., 1992. Measurement of the fracture energy using three-point bend tests Part 3-Influence of cutting the P-u tail. Materials and Structures, 25, pp. 327-334.

Hillerborg, A., Modeer, M., Petersson, P., 1976. Analysis of crack formation and crack growth in concrete by means of fracture mechanics and finite elements. Cement and Concrete. Research, 6.

Kim, H., Wagoner, M. P., Buttlar, W. G., 2009. Numerical fracture analysis on the specimen size dependency of asphalt concrete using a cohesive softening model. Construction and Building Materials, 23(5), pp. 2112-2120.

Olesen, J. F., Stang, H., 2006. Nonlinear fracture mechanics and plasticity of the split cylinder test. Materials and Structures, 39(4), 421-432.

OpenSees, 2008. Open System for Earthquake Engineering Simulation v1.7.5. Berkeley: Pacific Earthquake Engineering Research Center, University of California.

Rocco, C., Guinea, G., Planas, J., Elices, M., 1999a. Size effect and boundary conditions in the Brazilian test: Experimental verification. Materials and Structures, 32, 210-217.

Rocco, C., Guinea, G., Planas, J., Elices, M., 1999b. Size effect and boundary conditions in the brazilian test: theoretical analysis. Materials and Structures, 32, 437-444.

Rocco, C., Guinea, G., Planas, J., Elices, M., 2001. Review of the splitting-test standards from a fracture mechanics point of view. Cement and Concrete Research, 31(1), 73-82.

Sancho, J., Planas, J., Cendón, D., Reyes, E., Gálvez, J., 2007. An embedded crack model for finite element analysis of concrete. Engineering Fracture Mechanics, 74, 75-86.

Tang, T., 1994. Effects of load-distributed width on split tension of unnotched and notched cylindrical specimens. *Journal of testing and Evaluation*, 22(5), 401-409.

Timoshenko, S., Goodier, J. (1970). *Theory of Elasticity* (3rd editio.). McGraw-Hill Book Company.

Wagoner, M., Buttlar, W. G., Paulino, G. H., 2005. Disk-shaped Compact Tension Test for Asphalt Concrete Fracture. *Experimental Mechanics*, 45(3), 270-277.

Wu, R., Denneman, E., Harvey, J., 2009. Evaluation of an embedded discontinuity method for finite element analysis of hot mix asphalt concrete cracking. *Transportation Research Record*, 2127(530), 82-89.